

# An experimental and computational comparison of phosphorus- and selenium-based ligands for catalysis

Jamie S. Ritch and Bronte J. Charette

**Abstract:** To compare and contrast the bonding and reactivity of organoselenium ligands with organophosphines in coordination complexes, a new palladium(II) complex of the *Se,N*-chelating ligand *o*-(NH<sub>2</sub>)(X)C<sub>6</sub>H<sub>4</sub> (X = SePh, **2**) was prepared. Its characterization by NMR spectroscopy, single-crystal X-ray diffraction, and density functional theory calculations is contrasted with the Pd<sup>II</sup> complex of the related *P,N*-chelating ligand (X = PPh<sub>2</sub>, **1**). These techniques indicate that the phenylseleno moiety is a weaker  $\sigma$  donor to the PdCl<sub>2</sub> fragment than the diphenylphosphino group. Both complexes were suitable to catalyze the Suzuki–Miyaura coupling of *p*-tolylboronic acid and 4-bromobenzaldehyde.

**Key words:** organoselenium compounds, coordination chemistry, X-ray crystallography, density functional theory, Suzuki–Miyaura coupling.

**Résumé :** En vue d'effectuer une comparaison différentielle de ligands organoséléniés et d'organophosphines sur le plan de leurs propriétés de liaison et de leur réactivité dans des complexes de coordination, nous avons synthétisé un nouveau complexe de palladium(II) et du ligand chélateur à base de sélénium et d'azote *o*-(NH<sub>2</sub>)(X)C<sub>6</sub>H<sub>4</sub> (X = SePh, **2**). Nous avons caractérisé ce complexe par spectroscopie RMN, diffraction des rayons X sur cristal unique et calculs de la théorie de la fonctionnelle de la densité pour le comparer au complexe de Pd<sup>II</sup> et du ligand chélateur analogue à base de phosphore et d'azote (X = PPh<sub>2</sub>, **1**). Ces techniques indiquent que le groupement phényleseleno est un donneur  $\sigma$  plus faible envers le fragment PdCl<sub>2</sub> que le groupement diphenylphosphino. Par ailleurs, les deux complexes se sont révélés capables de catalyser le couplage de Suzuki–Miyaura entre l'acide *p*-tolylboronique et le 4-bromobenzaldéhyde. [Traduit par la Rédaction]

**Mots-clés :** composés organoséléniés, chimie de coordination, radiocristallographie, théorie de la fonctionnelle de la densité, couplage de Suzuki–Miyaura.

## Introduction

Rational ligand design is an essential tool for homogeneous catalysis research. Amongst the many reported ligand scaffolds, a common element for palladium-based catalysts is the incorporation of organophosphorus donors. Phosphines are valued for their strong  $\sigma$  donor ability in conjunction with the ability to act as a  $\pi$ -acid. Over the last several decades, there has been a growing interest in the use of selenoether-type ligands as alternatives to phosphines. Organoselenium ligands and their complexes to metals such as nickel, palladium, and rhodium are often air- and moisture-stable and have shown catalytic activity in a number of transformations including carbon–carbon coupling reactions.<sup>1</sup> Ligand synthesis often involves the use of an organic diselenide such as Ph<sub>2</sub>Se<sub>2</sub> with NaBH<sub>4</sub> to effect convenient selenylation of organic halides via a PhSe<sup>–</sup> equivalent.

A variety of scaffolds have been explored; some examples of multidentate hard–soft selenoether-containing ligands are illustrated in Chart 1. Palladium(II) complexes of the ligands **A**<sup>2</sup> and **B**<sup>3</sup> are effective Suzuki–Miyaura catalysts, while ligands **C**,<sup>4</sup> **D**,<sup>5</sup> and **E**<sup>6</sup> have been used to catalyze the Heck reaction. Ligand **D** is commercially available from Sigma-Aldrich and [(2,6-PhSeCH<sub>2</sub>)<sub>2</sub>C<sub>6</sub>H<sub>3</sub>]PdX] can also catalyze, for example, the boronation of allylic alcohols (X = Cl),<sup>7</sup> and the allylation of aldehydes with organotin reagents (X = OAc).<sup>8</sup> As further examples are reported, selenium-based catalysts

with activities surpassing even state-of-the-art phosphine-based systems have emerged.<sup>5</sup>

However, the reasons for such differences in activity are not well understood. The strong electron donor ability of selenium has been cited as an advantage of selenium-containing ligands; however, detailed electronic structure studies or direct comparisons between phosphine and selenoether ligands to this end remain rare. Additionally, the identity of the active catalyst is at times uncertain. In some systems, the Pd<sup>II</sup> coordination complex serves as a precatalyst that forms palladium selenide nanoparticles under thermal conditions, and these have been implicated as the source of Pd(0) particles (the “true catalyst”) for Heck transformations.<sup>9</sup> This does not, however, preclude single-site catalysis in other processes and mechanistic details are scant for many reported selenium-containing catalyst systems.

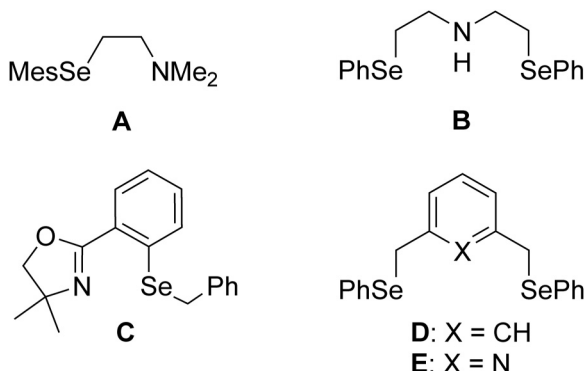
This contribution examines two [Pd(L)Cl<sub>2</sub>] complexes where L is either a chelating phosphine or selenoether ligand, both of which contain the same *ortho*-substituted aniline framework and differ only by the second heteroatom donor (–SePh or –PPh<sub>2</sub>). It is therefore possible to make a direct comparison of their structures, NMR properties, and  $\sigma$  donor ability. Additionally, their effectiveness as catalysts in a Suzuki–Miyaura coupling reaction is evaluated.

Received 25 August 2015. Accepted 3 November 2015.

**J.S. Ritch and B.J. Charette.** Department of Chemistry, The University of Winnipeg, 515 Portage Avenue, Winnipeg, MB R3B 2E9, Canada; Department of Chemistry, 360 Parker Building, University of Manitoba, Winnipeg, MB R3T 2N2, Canada.

**Corresponding author:** Jamie S. Ritch (email: [j.ritch@uwinnipeg.ca](mailto:j.ritch@uwinnipeg.ca)).

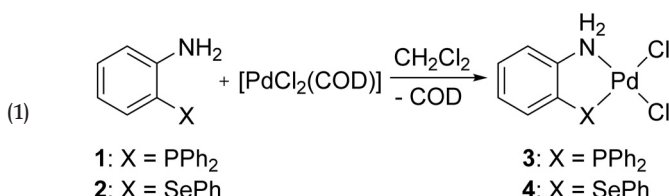
*This article is part of a Special Issue dedicated to celebrating the 50th Anniversary of the Department of Chemistry at the University of Calgary and to highlighting the chemical research being performed by faculty and alumni.*

**Chart 1.**

## Results and discussion

### Synthesis and NMR characterization of metal complexes

The ligands *o*-(NH<sub>2</sub>)(X)C<sub>6</sub>H<sub>4</sub> (**1**) (X = PPh<sub>2</sub>)<sup>10</sup> and **2** (X = SePh)<sup>11</sup> were prepared according to the reported procedures, from 2-fluoroaniline and 2-chloronitrobenzene, respectively. Palladium(II) complexes of the ligands were targeted to furnish diamagnetic complexes amenable to NMR studies and with a square-planar geometry for evaluation of the relative thermodynamic *trans*-effect of phosphorus and selenium donor sites. The chelating ligands were separately reacted with [PdCl<sub>2</sub>(COD)] (COD = 1,5-cyclooctadiene) in CH<sub>2</sub>Cl<sub>2</sub> at room temperature (eq. 1). The resultant complexes [PdCl<sub>2</sub>(*o*-(NH<sub>2</sub>)(X)C<sub>6</sub>H<sub>4</sub>)] (**3**) (X = PPh<sub>2</sub>) and **4** (X = SePh) precipitated from the reaction mixtures in high yields (83%–100%). The phosphine complex **3** has been previously prepared using another method and investigated as an anti-cancer agent,<sup>12</sup> while the selenoether complex **4** has not been reported. Complex **3** is a yellow solid, with no appreciable solubility in hydrocarbons, THF, Et<sub>2</sub>O, or CH<sub>2</sub>Cl<sub>2</sub>; it is sparingly soluble in hot MeCN and soluble in DMSO. Complex **4** is an orange solid that is similarly insoluble in common organic solvents, slightly more soluble than **3** in MeCN, and very soluble in DMSO.



Evidence of X,N-coordination in both cases was clearly observed by NMR spectroscopy. The <sup>31</sup>P NMR spectrum of **3** (d<sub>6</sub>-DMSO) indicates a singlet resonance shifted by +66.6 ppm compared to the free ligand **1**, and the NH<sub>2</sub> singlet resonance in the <sup>1</sup>H NMR spectrum is similarly shifted by +2.75 ppm. For the Se,N-complex **4**, the <sup>77</sup>Se NMR signal appears 178 ppm downfield of the signal for **2**. The NH<sub>2</sub> group, in addition to being significantly shifted by +2.40 ppm in the <sup>1</sup>H NMR spectrum compared to free ligand, also manifests as two closely spaced broad singlets with a separation of 13 Hz. This is consistent with two diastereotopic protons that are not rapidly exchanged on the NMR timescale, as would be expected for a square-planar complex featuring two stereochemically distinct faces. Here, the steric differentiation is provided by the SePh donor group, with a phenyl substituent projecting out of one side of the molecular plane and a lone pair out of the other. An interesting feature of the <sup>1</sup>H NMR spectrum of **4** is the visibility of low-intensity signals corresponding to the free ligand (those not overlapping with product signals). These resonances are observed even in recrystallized samples, suggesting a solution equilibrium in d<sub>6</sub>-DMSO (in the slow-exchange regime) where the solvent com-

petes with **2** for coordination to palladium rather than contamination by unreacted **2**. All resonances of the product spectrum become broadened at higher temperature, which seems to support this hypothesis. Additionally, in CD<sub>3</sub>CN, no signals for the free ligand are visible.

### X-ray crystallography

As the solid-state structure of **3** has not been previously reported and **4** is a new compound, we pursued X-ray quality single crystals of these complexes for diffraction studies. Suitable crystals of **3**-2DMSO and **4**-MeCN were grown in their respective solvents. Thermal ellipsoid plots are shown in Figs. 1 and 2; selected metrical parameters are presented in Table 1. The two structures are overall consistent with the solution-state NMR data, indicating square-planar palladium(II) chloride complexes of the *cis*-chelating ligands **1** and **2** (sum of angles around palladium: 360.1° and 360.2°, respectively). With the exception of the phenyl groups and amino protons, all atoms in complexes **3** and **4** are nearly coplanar — the largest deviations from planarity involve chlorine atoms. The PdCl<sub>2</sub> moiety is slightly twisted out of the mean plane in **3** (displacements of chlorine atoms +0.099 and -0.078 Å) and one chlorine atom in **4** is 0.095 Å from the mean plane. The selenium atom in complex **4** is chiral — the centrosymmetric structure contains a 1:1 mixture of enantiomers.

The Pd-Se distance in **4** is approximately 7% elongated compared to the Pd-P distance in **3**, consistent with the larger covalent radius of selenium. The lower s-character of the selenium-centred bonding orbitals is also borne out in the metrical data: the bond angles around selenium are noticeably smaller than those for phosphorus, e.g., the Pd-X-C<sub>phenyl</sub> angles for **3** and **4** are 101.31(6)° and 115.56(3)–118.94(10)°, respectively. Another notable feature of the X-ray data are the Pd-Cl distances: those distances *trans* to the NH<sub>2</sub> group in each complex are not significantly different (**3**: 2.3001(9) Å; **4**: 2.3017(5) Å), while those *trans* to phosphorus and selenium differ by approximately 0.03 Å (**3**: 2.3607(8) Å; **4**: 2.3352(5) Å). In the context of the thermodynamic *trans*-effect,<sup>13</sup> the Ph<sub>2</sub>P group is therefore observed to be a stronger σ donor than the PhSe group in the presently studied system. This is consistent with other findings that heavy chalcogenoethers are modest σ donors compared to organophosphines.<sup>14,15</sup>

Both crystal structures feature well-ordered lattice solvent molecules. In the (P,N) complex **3**, the NH<sub>2</sub> protons are each hydrogen bonded to one crystallographically unique DMSO molecule with N-H···O distances of 2.823(4) and 2.821(4) Å. This secondary bonding motif has been observed for related metal complexes, including the octahedral ruthenium(II) complex [RuCl<sub>2</sub>(**1**)(CO)<sub>2</sub>]·4DMSO<sup>16</sup> and the square-planar palladium(II) complex [PdCl<sub>2</sub>(4,5-dax)]·2DMSO (4,5-dax = 4,5-diaminoxylylene).<sup>17</sup> The crystal structure of (Se,N) complex **4** features a lattice acetonitrile molecule, but it does not engage in any significant secondary bonding interactions. The closest intermolecular contacts to the NH<sub>2</sub> protons in **4** are two N-H···Cl interactions (3.295(2) and 3.331(2) Å) generating a staircase-type packing arrangement (Fig. 3). With H···Cl distances of 2.53(3) and 2.54(3) Å, these contacts are in the range of “medium”-length hydrogen bonds involving metal-bound chlorine atoms.<sup>18</sup> No intermolecular Pd···Se interactions are detected.

### Computational studies

To probe the electronic structure of the related complexes **3** and **4**, DFT calculations were conducted on these structures using the M06 functional, which is corrected for dispersion and has been found to give more accurate bond lengths for transition metal complexes compared to nondispersion corrected functionals, e.g., B3LYP.<sup>19</sup> First to third row atoms were modeled using the 6-31G(d,p) basis set, whereas the cc-pVTZ basis set with SDB relativistic effective core potentials was used for palladium and selenium.

**Fig. 1.** Thermal ellipsoid plot (50% probability) of 3·DMSO; carbon-bound hydrogen atoms are omitted for clarity.

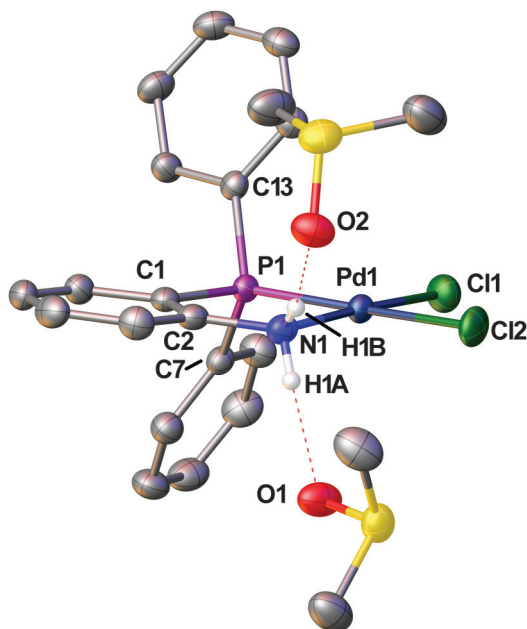


**Fig. 2.** Thermal ellipsoid plot (50% probability) of one enantiomer of complex 4·MeCN; carbon-bound hydrogen atoms and the lattice solvent molecule are omitted for clarity.

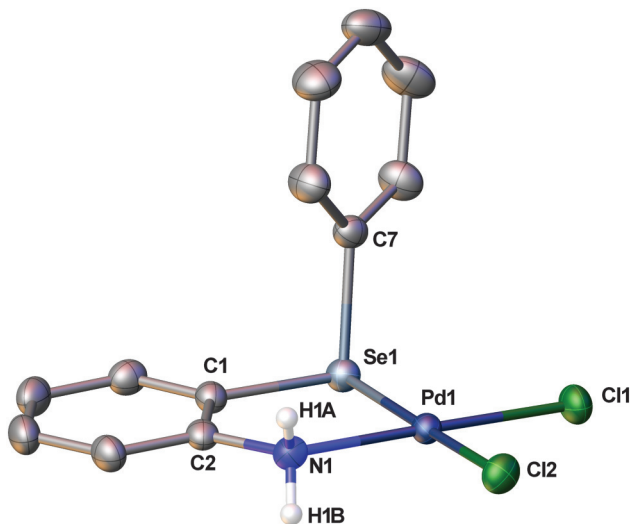
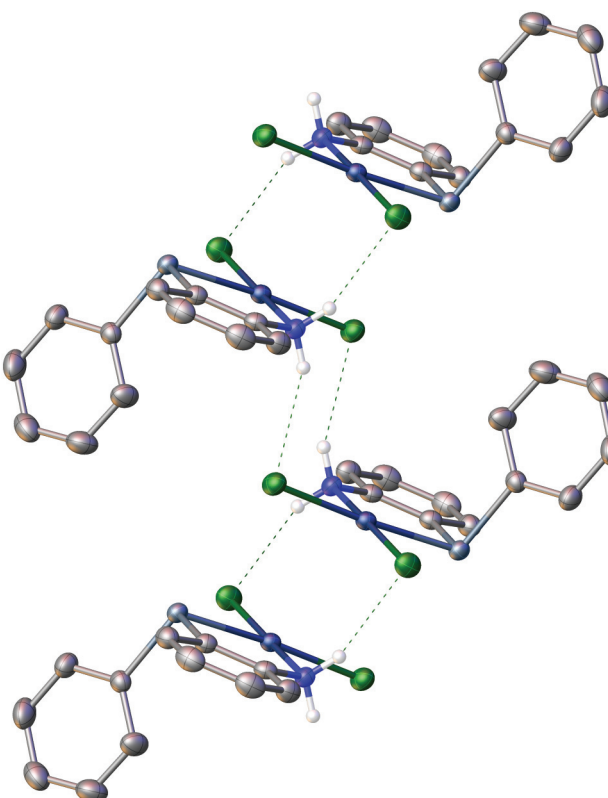


**Table 1.** Selected bond lengths ( $\text{\AA}$ ) and angles ( $^\circ$ ) for complexes [( $\text{o}-\text{NH}_2$ ) $\text{X}$ ] $\text{C}_6\text{H}_4$ PdCl<sub>2</sub>].

	X = PPh <sub>2</sub> (3)	X = SePh (4)
Pd1–N1	2.048(3)	2.0456(18)
Pd1–X1	2.2050(8)	2.3575(3)
Pd1–Cl1	2.3001(9)	2.3017(5)
Pd1–Cl2	2.3607(8)	2.3352(5)
X1–C1	1.806(3)	1.933(2)
N1–C2	1.458(4)	1.459(3)
Cl1–Pd1–Cl2	94.51(3)	94.18(2)
Pd1–X1–C7	118.94(10)	101.31(6)
Pd1–X1–C13	115.56(10)	
X1–Pd1–N1	85.61(8)	88.07(5)
X1–C1–C2–N1	3.3(4)	2.6(3)

**Fig. 3.** Packing diagram for complex 4 showing N–H···Cl hydrogen bonds.

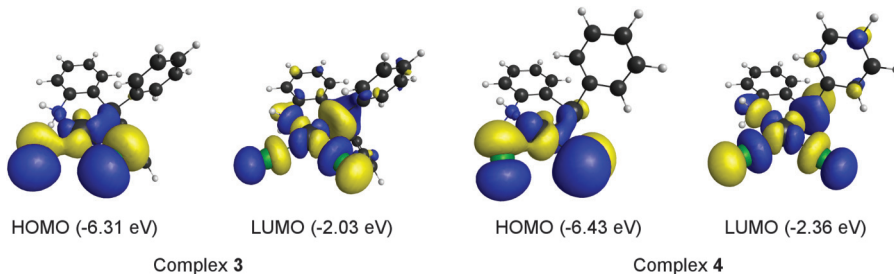
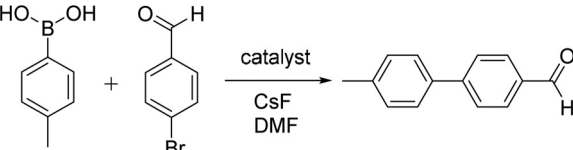


The optimized structures featured metrical parameters very similar to the crystal data, mainly differing by rotation of phenyl rings in the absence of crystal packing forces. Notably, the larger elongation of the Pd–Cl bond *trans* to phosphorus versus that *trans* to selenium is preserved in these gas-phase calculations (2.3450 versus 2.3177 Å), suggesting that the difference is unlikely due to a packing or hydrogen bonding effect. Analysis of the frontier orbitals (Fig. 4) indicated the HOMO compositions as mostly Cl(p), P(p), or Se(p) and Pd(d) orbital combinations, while the LUMOs also have larger contributions from N(p) and are  $\sigma$ -antibonding with respect to the PdL<sub>4</sub> square planes. HOMO–LUMO gaps of 4.28 eV for 3 and 4.07 eV for 4 are observed. The first ionization energies, estimated using Koopman's theorem, of 6.31 eV (3) and 6.43 eV (4) indicate that the phosphine complex is more susceptible to oxidation, as would be expected.<sup>20</sup>

Qualitative values of  $\Delta G_{rxn}^0$  for eq. 1 were estimated computationally in the gas phase (-62.5 kJ mol<sup>-1</sup> for 3 and +0.5 kJ mol<sup>-1</sup> for 4). The formation of the phosphine complex 3 is predicted to be more favourable than that of the selenoether complex 4 and hence ligand 1 is a stronger chelate ligand towards PdCl<sub>2</sub> relative to COD than 2. This is consistent with the higher *trans* influence of 1 versus 2 observed in the X-ray data as well as the experimental NMR spectral data for 4, which suggested dynamic behaviour involving some degree of dissociation of 2 in *d*<sub>6</sub>-DMSO solution.

### Catalysis experiments

To test the relative catalytic competencies of complexes 3 and 4, they were employed in the Suzuki–Miyaura coupling reaction of *p*-tolylboronic acid with 4-bromobenzaldehyde, utilizing conditions similar to those reported for the Cu<sup>I</sup>-catalyzed coupling of arylboronate esters with aryl iodides using the *P,N*-chelating ligand 1-<sup>t</sup>Bu<sub>2</sub>P-2-NMe<sub>2</sub>C<sub>6</sub>H<sub>4</sub>.<sup>21</sup> Conversion as measured by GC-MS was investigated for the two complexes, in addition to [PdCl<sub>2</sub>(COD)], under several reaction conditions (Table 2). DMF was used as the reaction solvent to ensure solubility of the catalyst.

**Fig. 4.** Frontier orbitals of complexes 3 and 4.**Table 2.** Comparative use of 3, 4, and [PdCl<sub>2</sub>(COD)] for a Suzuki–Miyaura coupling reaction.

Entry	Catalyst	Temperature (°C)	Time (h)	Yield (%)
1	None	120	14	9 <sup>a</sup>
2	[PdCl <sub>2</sub> (COD)]	120	14	>95%
3	<b>3</b>	120	14	>95%
4	<b>4</b>	120	14	>95%
5	[PdCl <sub>2</sub> (COD)]	50	14	35 <sup>a</sup>
6	<b>3</b>	50	14	20 <sup>a</sup>
7	<b>4</b>	50	14	36 <sup>a</sup>
8	[PdCl <sub>2</sub> (COD)]	23	14	24 <sup>a</sup>
9	<b>3</b>	23	14	13 <sup>a</sup>
10	<b>4</b>	23	14	13 <sup>a</sup>

Note: Conditions: boronic acid (0.1 mmol), aryl bromide (0.1 mmol), DMF (0.5 mL), catalyst (5 mol%), CsF (0.15 mmol).

<sup>a</sup>Yields measured by GC-MS versus the internal standard 4-nitrobenzaldehyde.

In the absence of a palladium complex, <10% conversion was observed at 120 °C, while 5 mol% of [PdCl<sub>2</sub>(COD)], **3**, or **4** affords quantitative conversion. At 50 °C, the selenium-containing complex **4** shows higher conversion than the phosphine complex **3** but does not outperform [PdCl<sub>2</sub>(COD)] and all complexes yield <50% conversion. Finally, at room temperature, no catalyst exceeds 25% conversion, and the COD complex reaches higher yields than both **3** and **4**, which are equal at 13%.

## Conclusions

The new palladium(II) complex (**4**) of a chelating organoseelenium ligand has been prepared and characterized by a number of methods to contrast its properties with the phosphine-ligated analogue **3**. Experimental evidence from <sup>1</sup>H NMR spectra and X-ray structural analysis indicates that the phenylselenyl substituent has a lower σ donor ability towards Pd<sup>II</sup> and ligand **2** is generally more weakly bound, which was corroborated computationally by DFT, including free energy calculations. Both complexes **3** and **4** are active catalysts in the Suzuki–Miyaura coupling of an arylboronic acid with an aryl bromide, albeit with activities not significantly higher than the simple COD complex of PdCl<sub>2</sub>.

Future studies will examine the donor ability of a wider range of selenium (and tellurium) donor ligands as compared to other heteroatoms such as nitrogen and phosphorus. The coordination chemistry of **2** towards other transition metals such as nickel and copper will be investigated to study their structures and reactivity, with the possibility of improving solubility of complexes through variation of the substitution patterns on the aromatic ring and selenium centre. Additionally, the mechanism of catalytic processes involving heavy chalcogenoethers will be probed computationally and experimentally.

## Experimental section

### General considerations

All manipulations were conducted under an inert atmosphere of argon using standard glovebox or Schlenk/vacuum line techniques, except where noted. The solvents dichloromethane, diethyl ether, and toluene (ACS grade) were sparged with argon and dried by passage through two columns of activated alumina before storage in PTFE-sealed glass vessels; diethyl ether was stored over sodium/benzophenone. Solvents were transferred by vacuum distillation into PTFE-sealed storage flasks over activated 4 Å molecular sieves for Schlenk manipulations. Acetonitrile was dried by stirring over CaH<sub>2</sub> overnight and then distilled onto activated 3 Å molecular sieves. *d*<sub>6</sub>-DMSO was dried over activated 4 Å molecular sieves and degassed using at least three freeze–pump–thaw cycles.

The reagents [PdCl<sub>2</sub>(COD)]<sup>22</sup> and *o*-(NH<sub>2</sub>)(X)C<sub>6</sub>H<sub>4</sub> (X = PPh<sub>2</sub>,<sup>10</sup> SePh<sup>11</sup>) were prepared according to the literature procedures. DMSO (anhydrous), *p*-tolylboronic acid, 4-bromobenzaldehyde, cesium fluoride, and 4-nitrobenzaldehyde were purchased from commercial sources and used as received. Melting points were recorded from samples sealed under argon in capillary tubes.

### Instrumentation

NMR spectra were collected on a Bruker 400 MHz Avance III spectrometer. Chemical shifts are reported in parts per million (ppm). <sup>1</sup>H and <sup>13</sup>C resonances are referenced to residual protons or carbon atoms in the deuterated solvent. For other nuclei, the external standards Ph<sub>2</sub>Se<sub>2</sub> in CDCl<sub>3</sub> (<sup>77</sup>Se) and H<sub>3</sub>PO<sub>4</sub>(aq) (<sup>31</sup>P) were utilized. Elemental analyses were performed by Canadian Microanalytical Ltd. (Delta, British Columbia, Canada). GC-MS analysis was conducted using an Agilent 5975C system. High-resolution mass spectra (HRMS) were obtained using a quadrupole ion trap mass spectrometer with electrospray ionization (ESI).

### Synthesis of 3

To a mixture of ligand **1** (168 mg, 0.61 mmol) and [PdCl<sub>2</sub>(COD)] (157 mg, 0.55 mmol) was added CH<sub>2</sub>Cl<sub>2</sub> (25 mL). The yellow solution was stirred for 1 h at room temperature, during which time a yellow precipitate formed. The volatiles were removed in vacuo, and the resultant solid was washed with Et<sub>2</sub>O (3 × 5 mL). After drying in vacuo, **3** was obtained as a yellow powder in quantitative yield. Solution <sup>1</sup>H and <sup>31</sup>P NMR spectral data in *d*<sub>6</sub>-DMSO matched that reported in the literature.<sup>12</sup> Anal. calcd. (%): C 47.55, H 3.55, N 3.08; found: C 47.38, H 3.41, N 3.09. An X-ray quality single crystal of **3**-2DMSO was grown from a layered DMSO-toluene solution at room temperature.

### Synthesis of 4

Complex **4** was prepared in a method analogous to that used for complex **3** using ligand **2** (162 mg, 0.65 mmol) and [PdCl<sub>2</sub>(COD)] (171 mg, 0.60 mmol) and isolated as an orange powder (211 mg, 83%, mp > 240 °C (dec.)). <sup>1</sup>H NMR (*d*<sub>6</sub>-DMSO) δ: 7.88–7.68 (overlapping m and d, *J*<sub>HH</sub>(d) = 13 Hz, 4H, aromatic CH (m) and NH<sub>2</sub> (d)), 7.61–7.37 (m, 7H, aromatic CH); low-intensity resonances corresponding to approximately 12% free ligand **2** were observed at δ 7.27–7.13 (m, aromatic CH), 6.82 (d, *J*<sub>HH</sub> = 8 Hz, aromatic CH), 6.54

**Table 3.** Crystallographic Data for **3**·2DMSO and **4**·MeCN.

Compound	<b>3</b> ·2(C <sub>2</sub> H <sub>6</sub> OS)	<b>4</b> ·C <sub>2</sub> H <sub>3</sub> N
Empirical formula	C <sub>22</sub> H <sub>28</sub> Cl <sub>2</sub> NO <sub>2</sub> PPdS <sub>2</sub>	C <sub>14</sub> H <sub>14</sub> N <sub>2</sub> Cl <sub>2</sub> SePd
Formula weight	610.84	466.53
Temperature (K)	193(2)	193(2)
Crystal system	Monoclinic	Monoclinic
Space group	P2 <sub>1</sub> /n	P2 <sub>1</sub> /c
<i>a</i> (Å)	10.9748(6)	10.7926(6)
<i>b</i> (Å)	18.4224(10)	7.3379(4)
<i>c</i> (Å)	13.0833(7)	20.5576(12)
$\alpha$ (°)	90	90
$\beta$ (°)	105.6894(7)	99.4615(7)
$\gamma$ (°)	90	90
Volume (Å <sup>3</sup> )	2546.7(2)	1605.91(16)
<i>Z</i>	4	4
<i>D</i> <sub>calcd.</sub> (g cm <sup>-3</sup> )	1.593	1.93
$\mu$ (mm <sup>-1</sup> )	1.185	3.745
<i>F</i> (000)	1240	904
Crystal size (mm <sup>3</sup> )	0.335×0.082×0.041	0.446×0.192×0.09
Radiation	MoK <sub>α</sub> ( $\lambda$ = 0.71073 Å)	MoK <sub>α</sub> ( $\lambda$ = 0.71073 Å)
$\theta$ range for data collection (°)	1.959–27.6	1.913–28.25
Index ranges	-14 ≤ <i>h</i> ≤ 14, -23 ≤ <i>k</i> ≤ 23, -16 ≤ <i>l</i> ≤ 16	-14 ≤ <i>h</i> ≤ 12, -9 ≤ <i>k</i> ≤ 9, -27 ≤ <i>l</i> ≤ 27
Reflections collected	21623	11808
Independent reflections	5876 ( <i>R</i> <sub>int</sub> = 0.0434)	3864 ( <i>R</i> <sub>int</sub> = 0.0202)
Data/restraints/parameters	5876/2/292	3864/0/190
Goodness-of-fit on <i>F</i> <sup>2</sup>	1.04	1.04
Final <i>R</i> indexes ( <i>I</i> > 2σ( <i>I</i> ))	<i>R</i> <sub>1</sub> = 0.0364, <i>wR</i> <sub>2</sub> = 0.0875	<i>R</i> <sub>1</sub> = 0.0210, <i>wR</i> <sub>2</sub> = 0.0518
Final <i>R</i> indexes (all data)	<i>R</i> <sub>1</sub> = 0.0498, <i>wR</i> <sub>2</sub> = 0.0959	<i>R</i> <sub>1</sub> = 0.0245, <i>wR</i> <sub>2</sub> = 0.0534
Largest diff. peak/hole (e Å <sup>-3</sup> )	1.18/-0.59	0.57/-0.45

(*t*, *J*<sub>HH</sub> = 8 Hz, aromatic CH), and 5.32 (br s, NH<sub>2</sub>). <sup>13</sup>C{<sup>1</sup>H} NMR (*d*<sub>6</sub>-DMSO) δ: 147.3 (s), 137.9\* (s), 133.5 (s), 131.6\* (s), 131.2 (s), 130.7 (s), 130.2 (s), 129.4\* (s), 128.8 (s), 128.1 (s), 126.3\* (s), 125.7 (s); resonances marked with an asterisk match <sup>13</sup>C chemical shifts for the free ligand **2**. Of these four resonances (of 12 total), two are likely overlapping signals from **2** and **4** and two are from **2**.

<sup>77</sup>Se{<sup>1</sup>H} NMR (*d*<sub>6</sub>-DMSO) δ: 482. HRMS (ESI) *m/z*: [M + Na]<sup>+</sup> calcd. for C<sub>12</sub>H<sub>11</sub>Cl<sub>2</sub>NPdSeNa: 447.83608; found: 447.83519. Anal. calcd. (%): C 33.87, H 2.61, N 3.29; found: C 33.21, H 2.43, N 3.25. An X-ray quality single crystal of **4**·MeCN was grown from a slowly cooled concentrated solution of the complex in warm acetonitrile.

### X-ray crystallography

Data were collected for a suitable crystal of each complex with a Bruker APEX-II CCD diffractometer at 193 K using APEX2.<sup>23</sup> Cell refinement and data reduction were carried out using SAINT,<sup>24</sup> and numerical absorption correction was applied using SAD-ABS.<sup>25</sup> Using Olex2,<sup>26</sup> the structure was solved with the SHELXS<sup>27</sup> structure solution program using the Patterson method for **3** and direct methods for **4**. Least squares refinement of the structure was carried out against *F*<sup>2</sup> using SHELXL.<sup>28</sup> The structures were well ordered and no special considerations were needed for the refinements. Carbon-bound hydrogen atoms were placed in calculation positions and treated in a riding-model approximation, while nitrogen-bound hydrogen atoms were located in the difference electron map and allowed to refine isotropically. The N-H hydrogen atoms in **3** were restrained to a length of 0.89 Å. All nonhydrogen atoms were modeled anisotropically. Selected crystal data are given in Table 3.

### General procedure for catalytic reactions

In a glovebox, boronic acid (0.1 mmol), aryl halide (0.1 mmol), cesium fluoride (0.15 mmol), and catalyst (5 mol%) were weighed into a vial equipped with a stir bar. Dimethylformamide was added (0.5 mL) and the vial was sealed with a PTFE-lined screw cap. The vial was heated to the reaction temperature for 14 h. After cooling to room temperature, an internal standard (4-nitrobenzaldehyde, 20 μL of a 0.5 mol L<sup>-1</sup> solution in acetonitrile)

was added and the reaction mixture was diluted with ethyl acetate (2 mL), filtered through a plug of silica gel in a Pasteur pipet, and analyzed by EI GC-MS. Reaction conversion were determined by integration of the total ion current and using the separately determined relative response factors of the product and internal standard.

### DFT calculations

Starting from crystal structure coordinates, gas-phase closed-shell geometry optimizations of complexes **3** and **4** were performed with GAMESS<sup>29</sup> using the M06 functional.<sup>30</sup> The 6-31G(d,p) basis set was used for carbon, hydrogen, nitrogen, and phosphorus, while relativistic effective core potentials as implemented in SDB-cc-pVTZ were applied to selenium and palladium.<sup>31</sup> Molecular orbital plots were generated at a contour level of 0.03 using wxMacMolPlt.<sup>32</sup>

### Supplementary material

Supplementary material is available with the article through the journal Web site at <http://nrcresearchpress.com/doi/suppl/10.1139/cjc-2015-0417>. Further computational details, including coordinates for optimized geometries, are tabulated in the supplementary material. CCDC 1414987–1414988 contain the supplementary crystallographic data for this paper. These data can be obtained, free of charge, via [www.ccdc.cam.ac.uk/conts/retrieving.html](http://www.ccdc.cam.ac.uk/conts/retrieving.html) (or from the Cambridge Crystallographic Data Centre, 12 Union Road, Cambridge CB2 1EZ, UK (Fax: 44-1223-336033 or e-mail: [deposit@ccdc.cam.ac.uk](mailto:deposit@ccdc.cam.ac.uk))).

### Acknowledgements

Financial support from the University of Winnipeg, an adjunct appointment in the Department of Chemistry, University of Manitoba, and supercomputing resources from Compute Canada and Westgrid are gratefully acknowledged. The authors thank Bob McDonald (X-ray Crystallography Laboratory, Department of Chemistry, University of Alberta) for single-crystal X-ray diffraction data collection and Dr. Jiaxi Wang (Mass Spectrometry Facility, Queen's University) for ESI HRMS analysis. Dr. Joshua Hollett

(Department of Chemistry, The University of Winnipeg) is thanked for useful discussions regarding DFT calculations.

## References

- (1) Kumar, A.; Rao, G. K.; Saleem, F.; Singh, A. K. *Dalton Trans.* **2012**, 41 (39), 11949. doi:[10.1039/c2dt31198d](https://doi.org/10.1039/c2dt31198d).
- (2) Paluru, D. K.; Dey, S.; Wadawale, A.; Maity, D. K.; Bhuvanesh, N.; Jain, V. K. *Eur. J. Inorg. Chem.* **2015**, 2015 (3), 397. doi:[10.1002/ejic.201402943](https://doi.org/10.1002/ejic.201402943).
- (3) Kumar, S.; Rao, G. K.; Kumar, A.; Singh, M. P.; Singh, A. K. *Dalton Trans.* **2013**, 42 (48), 16939. doi:[10.1039/c3dt51658j](https://doi.org/10.1039/c3dt51658j).
- (4) Chakraborty, T.; Srivastava, K.; Singh, H. B.; Butcher, R. J. *J. Organomet. Chem.* **2011**, 696 (13), 2559. doi:[10.1016/j.jorganchem.2011.03.047](https://doi.org/10.1016/j.jorganchem.2011.03.047).
- (5) Yao, Q.; Kinney, E. P.; Zheng, C. *Org. Lett.* **2004**, 6 (17), 2997. doi:[10.1021/o10486977](https://doi.org/10.1021/o10486977).
- (6) Das, D.; Rao, G. K.; Singh, A. K. *Organometallics* **2009**, 28 (20), 6054. doi:[10.1021/om900570g](https://doi.org/10.1021/om900570g).
- (7) Olsson, V. J.; Sebelius, S.; Selander, N.; Szabó, K. J. *J. Am. Chem. Soc.* **2006**, 128 (14), 4588. doi:[10.1021/ja060468n](https://doi.org/10.1021/ja060468n).
- (8) Yao, Q.; Sheets, M. J. *Org. Chem.* **2006**, 71 (14), 5384. doi:[10.1021/jo060456k](https://doi.org/10.1021/jo060456k).
- (9) Singh, P.; Das, D.; Prakash, O.; Singh, A. K. *Inorganica Chim. Acta* **2013**, 394, 77. doi:[10.1016/j.ica.2012.07.029](https://doi.org/10.1016/j.ica.2012.07.029).
- (10) Seipel, K. R.; Platt, Z. H.; Nguyen, M.; Holland, A. W. *J. Org. Chem.* **2008**, 73 (11), 4291. doi:[10.1021/jo8001497](https://doi.org/10.1021/jo8001497).
- (11) Deobald, A. M.; Simon de Camargo, L. R.; Tabarelli, G.; Hörner, M.; Rodrigues, O. E. D.; Alves, D.; Braga, A. L. *Tetrahedron Lett.* **2010**, 51 (26), 3364. doi:[10.1016/j.tetlet.2010.04.076](https://doi.org/10.1016/j.tetlet.2010.04.076).
- (12) Chatterjee, S.; Hockless, D. C. R.; Salem, G.; Waring, P. J. *Chem. Soc. Dalton Trans.* **1997**, (20), 3889. doi:[10.1039/A704083K](https://doi.org/10.1039/A704083K).
- (13) Pidcock, A.; Richards, R. E.; Venanzi, L. M. *J. Chem. Soc. Inorg. Phys. Theor.* **1966**, (0), 1707. doi:[10.1039/JI96600001707](https://doi.org/10.1039/JI96600001707).
- (14) Levason, W.; Orchard, S. D.; Reid, G. *Coord. Chem. Rev.* **2002**, 225 (1-2), 159. doi:[10.1016/S0010-8545\(01\)00412-X](https://doi.org/10.1016/S0010-8545(01)00412-X).
- (15) Murray, S. G.; Hartley, F. R. *Chem. Rev.* **1981**, 81 (4), 365. doi:[10.1021/cr00044a003](https://doi.org/10.1021/cr00044a003).
- (16) Lee, C.-C.; Liu, Y.-H.; Peng, S.-M.; Chou, P.-T.; Chen, J.-T.; Liu, S.-T. *Polyhedron* **2012**, 35 (1), 23. doi:[10.1016/j.poly.2011.12.032](https://doi.org/10.1016/j.poly.2011.12.032).
- (17) Pérez-Cabré, M.; Cervantes, G.; Moreno, V.; Prieto, M. J.; Pérez, J. M.; Font-Bardia, M.; Solans, X. *J. Inorg. Biochem.* **2004**, 98 (3), 510. doi:[10.1016/j.jinorgbio.2003.12.022](https://doi.org/10.1016/j.jinorgbio.2003.12.022).
- (18) Aullón, G.; Bellamy, D.; Orpen, A. G.; Brammer, L.; Bruton, E. A. *Chem. Commun.* **1998**, (6), 653. doi:[10.1039/A709014E](https://doi.org/10.1039/A709014E).
- (19) Minenkov, Y.; Singstad, Å.; Occhipinti, G.; Jensen, V. R. *Dalton Trans.* **2012**, 41 (18), 5526. doi:[10.1039/c2dt12232d](https://doi.org/10.1039/c2dt12232d).
- (20) Ogura, F.; Yamaguchi, H.; Otsubo, T.; Tanaka, H. *Bull. Chem. Soc. Jpn.* **1982**, 55 (2), 641. doi:[10.1246/bcsj.55.641](https://doi.org/10.1246/bcsj.55.641).
- (21) Gurung, S. K.; Thapa, S.; Kafle, A.; Dickie, D. A.; Giri, R. *Org. Lett.* **2014**, 16 (4), 1264. doi:[10.1021/o1500310u](https://doi.org/10.1021/o1500310u).
- (22) Drew, D.; Doyle, J. R.; Shaver, A. G. In *Inorganic Syntheses*; Cotton, F. A., Ed.; John Wiley & Sons, Inc., 1972; pp. 47–55.
- (23) APEX2; Bruker AXS Inc.: Madison, WI, 2013.
- (24) SAINT; Bruker AXS Inc.: Madison, WI, 2013.
- (25) SADABS; Bruker AXS Inc.: Madison, WI, 2013.
- (26) Dolomanov, O. V.; Bourhis, L. J.; Gildea, R. J.; Howard, J. A. K.; Puschmann, H. J. *Appl. Crystallogr.* **2009**, 42 (2), 339. doi:[10.1107/S0021889808042726](https://doi.org/10.1107/S0021889808042726).
- (27) Sheldrick, G. M. *Acta Crystallogr.* **2008**, A64 (1), 112. doi:[10.1107/S0108767307043930](https://doi.org/10.1107/S0108767307043930).
- (28) Sheldrick, G. M. *Acta Crystallogr. Sect. C Struct. Chem.* **2015**, 71 (1), 3. doi:[10.1107/S2053229614024218](https://doi.org/10.1107/S2053229614024218).
- (29) Schmidt, M. W.; Baldridge, K. K.; Boatz, J. A.; Elbert, S. T.; Gordon, M. S.; Jensen, J. H.; Koseki, S.; Matsunaga, N.; Nguyen, K. A.; Su, S.; Windus, T. L.; Dupuis, M.; Montgomery, J. A. *J. Comput. Chem.* **1993**, 14 (11), 1347. doi:[10.1002/jcc.54014112](https://doi.org/10.1002/jcc.54014112).
- (30) Zhao, Y.; Truhlar, D. G. *Theor. Chem. Acc.* **2007**, 120 (1–3), 215. doi:[10.1007/s00214-007-0310-x](https://doi.org/10.1007/s00214-007-0310-x).
- (31) Martin, J. M. L.; Sundermann, A. *J. Chem. Phys.* **2001**, 114 (8), 3408. doi:[10.1063/1.1337864](https://doi.org/10.1063/1.1337864).
- (32) Bode, B. M.; Gordon, M. S. *J. Mol. Graph. Model.* **1998**, 16 (3), 133. doi:[10.1016/S1093-3263\(99\)00002-9](https://doi.org/10.1016/S1093-3263(99)00002-9).